THE JOURNAL OF PHYSICAL CHEMISTRY Letters

Letter

Cite This: J. Phys. Chem. Lett. 2019, 10, 1382−1387

pubs.acs.org/JPCL

Tracing the 267 nm-Induced Radical Formation in Dimethyl Disulfide Using Time-Resolved X-ray Absorption Spectroscopy

Kirsten Schnorr,*[,†,‡] Aditi Bhattacherjee,[†,‡] Katherine J. Oosterbaan,[†,‡] Mickaël G. Delcey,[†,‡] Zheyue Yang,[†,‡] Tian Xue,[†,‡] Andrew R. Attar,[†,‡] Adam S. Chatterley,[†,‡] Martin Head-Gordon,[†,‡] Stephen R. Leone,[†,‡,¶] and Oliver Gessner*[,‡]

[†]Department of Chemistry, University of California, Berkeley, California 94720, United States

[‡]Chemical Sciences Division, Lawrence Berkeley National Laboratory, Berkeley, California 94720, United States

[¶]Department of Physics, University of California, Berkeley, California 94720, United States

Supporting Information

ABSTRACT: Disulfide bonds are pivotal for the structure, function, and stability of proteins, and understanding ultraviolet (UV)-induced S−S bond cleavage is highly relevant for elucidating the fundamental mechanisms underlying protein photochemistry. Here, the near-UV photodecomposition mechanisms in gas-phase dimethyl disulfide, a prototype system with a S−S bond, are probed by ultrafast transient X-ray absorption spectroscopy. The evolving electronic structure during and after the dissociation is simultaneously monitored at the sulfur $L_{1,2,3}$-edges and the carbon K-edge with 100 fs (FWHM) temporal resolution using the broadband soft X-ray spectrum from a femtosecond high-order harmonics light source. Dissociation products are identified with the help of ADC and RASPT2 electronic-structure calculations. Rapid dissociation into two CH_3S radicals within 120 ± 30 fs is identified as the major relaxation pathway after excitation with 267 nm radiation. Additionally, a 30 ± 10% contribution from asymmetric CH_3S_2 + CH_3 dissociation is indicated by the appearance of CH_3 radicals, which is, however, at least partly the result of multiphoton excitation.

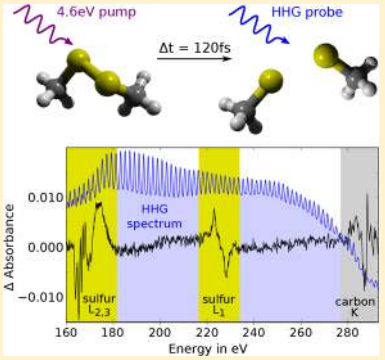

Disulfide bonds play a crucial role for regulating the structure, function, and stability of multiple proteins and enzymes.[1] When exposed to ultraviolet (UV) light, efficient S−S bond rupture can occur, leading to different protein tertiary structures and the reduction or even loss of biological functions.[2,3] Studying UV-induced cleavage of disulfide bonds in real time is pivotal to understanding the fundamental mechanisms of protein photodamage and photorepair. Thiyl radicals, for example, the highly reactive primary products of S−S bond rupture, are not well characterized because of their transient nature. Standard techniques for studying radicals such as electron paramagnetic resonance (EPR) spectroscopy are insensitive to sulfur because of its large spin−orbit coupling parameter.[4,5] Here, radical formation from gaseous dimethyl disulfide (DMDS, $H_3C−S−S−CH_3$) after excitation with 267 nm radiation is probed by broadband femtosecond transient X-ray absorption spectroscopy (fs-TRXAS), simultaneously monitoring the UV-induced dynamics at the sulfur $L_{1,2,3}$- and carbon K-edges.

Previous experiments using chemical analytic methods,[6] ion time-of-flight,[7] UV absorption spectroscopy,[8] and photoelectron detection[9] observed predominantly dissociation into two methyl-thiyl (CH_3S) radicals after UV excitation between 230 and 266 nm. In contrast, resonance Raman spectroscopy[10] of gas-phase DMDS and a very recent picosecond sulfur K-edge TRXAS of DMDS in solution,[11] both using 266 nm excitation, indicated predominant scission of a C−S bond, although secondary reactions could play a role. The fs-TRXAS results presented here, in combination with electronic-structure calculations on the ADC and RASPT2 level for spectral assignment, show that gas-phase DMDS, excited with a 267 nm photon, predominantly undergoes fast direct dissociation into two CH_3S radicals within 120 ± 30 fs, providing a definitive assignment of the initial pathway: The S−S bond cleavage is triggered by the promotion of a nonbonding sulfur electron to the antibonding σ^*_{SS} orbital. C−S bond cleavage is also observed, albeit with a smaller yield and at least partly ascribed to multiphoton-induced processes.

In the experiment, gas-phase DMDS molecules are excited with 267 nm pump pulses using fluences of 8, 28, and 96 mJ/cm^2, in the following referred to as low, intermediate, and high, respectively. UV-induced dynamics are monitored by recording the time-dependent changes in X-ray absorption using broadband (160−300 eV) pulses from a table-top high-harmonic generation (HHG) light source covering both the carbon K and sulfur $L_{1,2,3}$ absorption edges. High-level electronic-structure calculations are carried out for X-ray spectral assignment at the ADC level[12] with the cc-pCVDZ

Received: January 18, 2019
Accepted: March 5, 2019
Published: March 5, 2019

DOI: 10.1021/acs.jpclett.9b00159
J. Phys. Chem. Lett. 2019, 10, 1382−1387

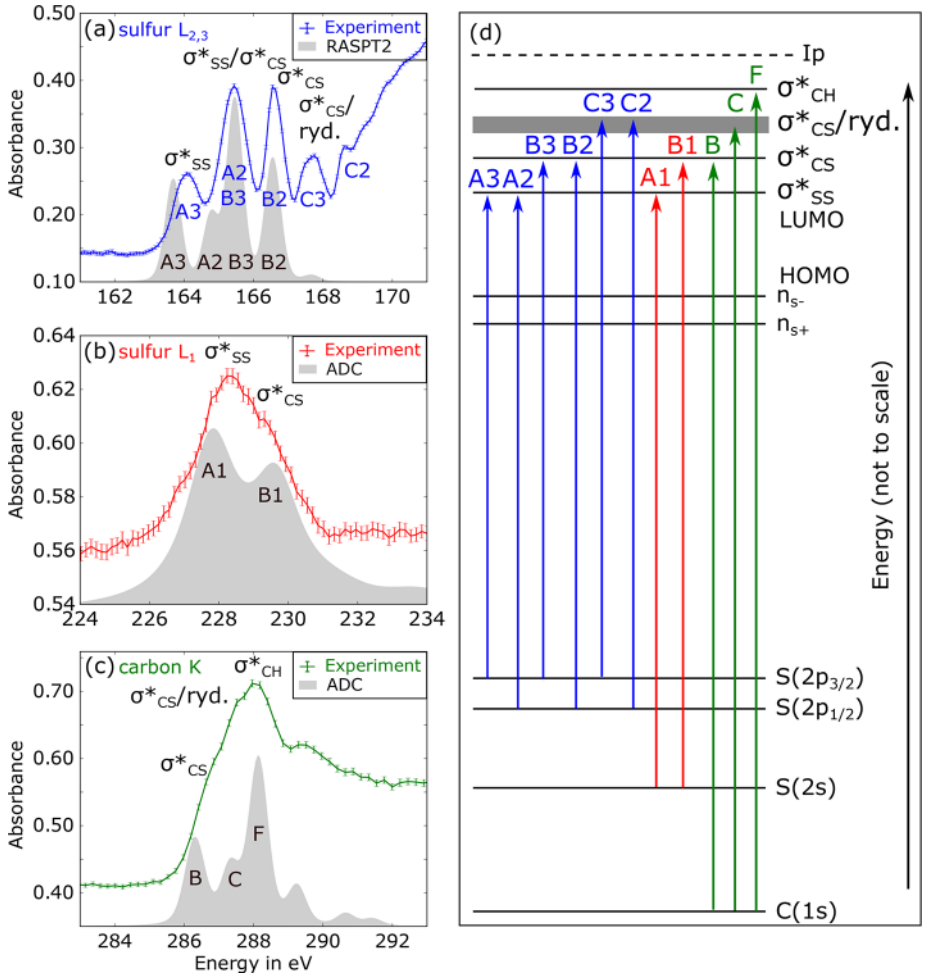

Figure 1. Experimental (colored) and calculated (gray shaded) absorption spectra of DMDS at the (a) sulfur $L_{2,3}$-edge, (b) sulfur L_1-edge, and (c) carbon K-edge. (d) Inner-shell transitions leading to the population of σ^*_{SS} (A), σ^*_{CS} (B), and σ^*_{CH} (F). The σ^*_{CS}/ryd. manifold (C) is drawn as a broad line to indicate that several orbitals may contribute.

basis set[13,14] for the sulfur L_1- and carbon K-edges and at the RASPT2[15,16] level with the ANO-RCC-VTZP[17] basis set for the sulfur $L_{2,3}$-edge, whereby the spin−orbit coupling was estimated using the RASSI-SO method.[18] UV absorption spectra are calculated at the CASPT2 level. Details of the setup, data acquisition, analysis, and calculations are provided in the Supporting Information.

Ground-state DMDS X-ray absorption spectra recorded at the sulfur $L_{2,3}$-, L_1- and carbon K-edges are shown in panels a, b, and c of Figure 1, respectively, together with corresponding calculated spectra (gray shaded, see Table S1 for peak assignments and positions). The core-to-valence transition labels contain a letter indicating the valence orbital (A, σ^*_{SS}; B, σ^*_{CS}; C, σ^*_{CS}/ryd.; F, σ^*_{CH}) and, for the sulfur L-edges, a number indicating the core orbital involved in the transition (1, S(2s); 2, S($2p_{1/2}$); or 3, S($2p_{3/2}$)). The lowest-energy excitation A3, for example, is assigned to the S($2p_{3/2}$) → σ^*_{SS} transition at the sulfur $L_{2,3}$-edge. The second peak A2/B3 contains two transitions, S($2p_{1/2}$) → σ^*_{SS} and S($2p_{3/2}$) → σ^*_{CS}. Peak B2 is attributed to S($2p_{1/2}$) → σ^*_{CS} excitations. The assignments are based on RASPT2 calculations and agree with previous studies.[19] According to the ADC calculations, peaks C3 and C2 are associated with excitations to higher-lying orbitals of mixed σ^*_{CS}/Rydberg character (σ^*_{CS}/ryd.). The distinct shoulder around 172 eV in Figure 2a likely originates from a shape resonance (SR) associated with the population of higher-lying orbitals, such as S(5s) and S(3d), as observed in a previous sulfur K-edge study.[20] The sharp increase in absorbance for energies beyond peak C2 is a rising edge due to ionization. The sulfur L_1-edge spectrum (Figure 1b) consists of two partially overlapping peaks A1 and B1, corresponding to S(2s) → σ^*_{SS} and S(2s) → σ^*_{CS} transitions, respectively. The experimental carbon K-edge spectrum in Figure 1c is dominated by a broad peak with low-energetic shoulders, consisting of transitions from C(1s) core to σ^*_{CS} (B), σ^*_{CS}/ryd. (C), and σ^*_{CH} (F) orbitals, as shown in the calculated spectrum (Figure 1c).

Pump−probe spectra are recorded for delays up to 100 ps, but all dynamic features rise or decay within 300 fs or less (Figure S4). Figure 2a shows the X-ray absorption spectra of ground-state DMDS (gray) and of the excitation products (red) integrated over a delay range of 300−2000 fs. Dissociation products are analyzed by comparing the measured spectra (Figure 2b,c,d) with calculated CH_3S and CH_3S_2 + CH_3 radical spectra (Figures 2e,f,g). Transitions to orbitals that are present in both DMDS and radical fragments carry the same labels. For CH_3S_2, the two sulfur atoms become distinguishable as indicated by subscripts 1 and 2 (inset Figure 2a). New resonances, not present in DMDS, are labeled with additional capital letters (D, S(3p); E, C(2p)). The peak assignments and positions are summarized in Table S2.

DOI: 10.1021/acs.jpclett.9b00159
J. Phys. Chem. Lett. 2019, 10, 1382−1387

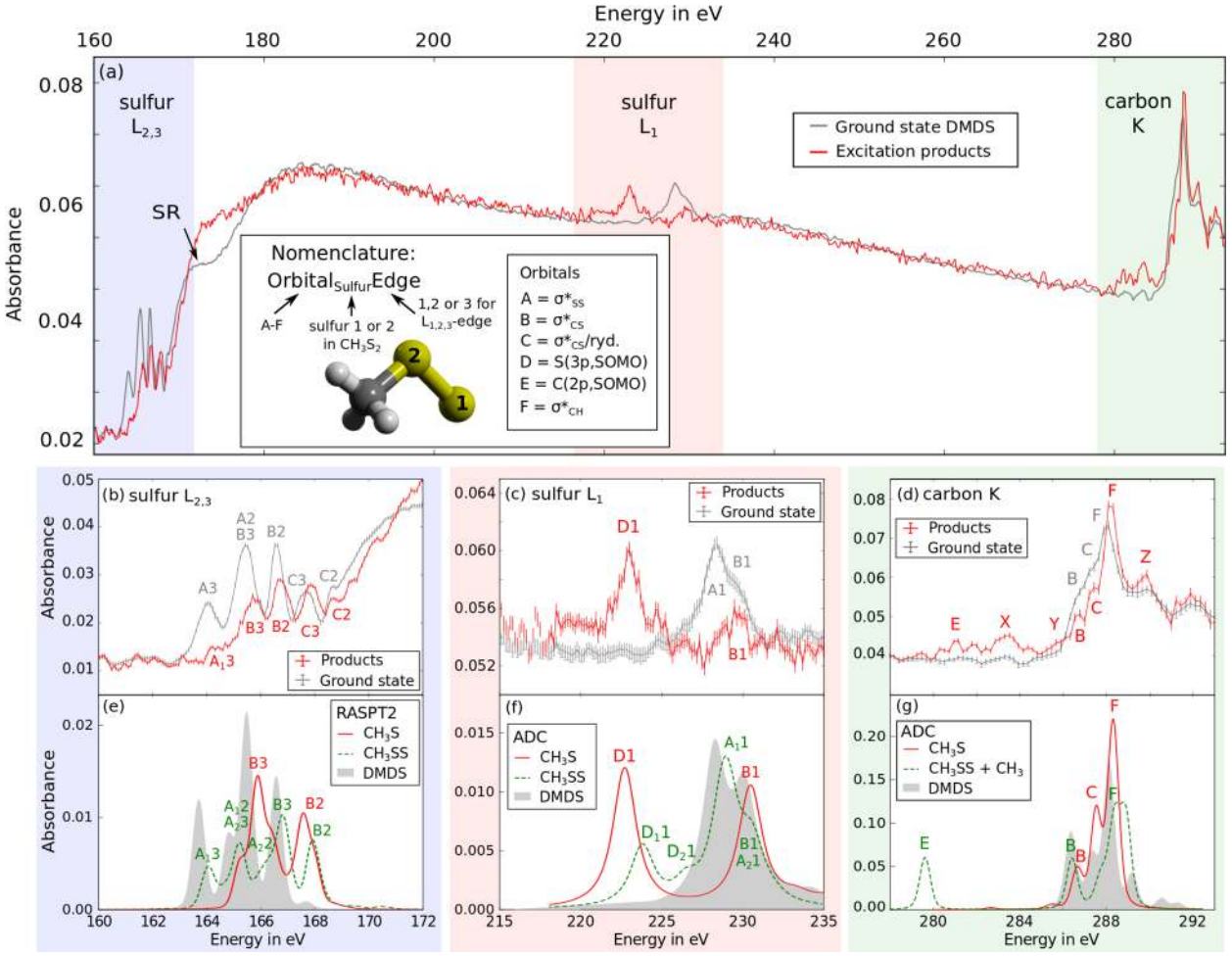

Figure 2. (a) Measured absorption spectra of ground-state DMDS (gray) and reaction products (red) after 267 nm excitation. The ground-state spectrum is scaled by a factor of 0.14 that corresponds to the amount of UV-excited DMDS molecules for low pump fluence. The inset summarizes the peak nomenclature. SR marks the shape resonance, which is not included in the magnified views in panels b–d. (e–g) Calculated absorption spectra for CH_3S (red solid lines), CH_3S_2 + CH_3 (dashed green lines), and DMDS (gray shaded) at (e) the sulfur $L_{2,3}$-edge, (f) the sulfur L_1-edge, and (g) the carbon K-edge. CH_3S spectra are multiplied by a factor of 2 to account for the breakup into two radicals.

The most pronounced photoinduced spectral changes are associated with transitions originating from sulfur 2s- and 2p-orbitals. At the sulfur $L_{2,3}$-edge (Figure 2b), peak A3 is almost entirely depleted, peaks B3 and B2 are strongly suppressed, and all absorption features are blue-shifted by 0.2–0.4 eV. A comparison to the calculated DMDS ground-state (gray) and CH_3S radical (red) spectra in Figure 2e qualitatively reproduces these trends. In particular, the strong suppression of peaks A3 and A2 (the latter partly obscured by peak B3) in the product spectrum is consistent with S–S bond rupture because these signals correspond to excitations to σ^*_{SS} orbitals associated with this bond. In contrast, the calculated CH_3S_2 radical spectrum (dashed green) exhibits clear σ^*_{SS} excitation features ($A_{1,2}2,3$). Features B3 and B2 are roughly a factor of two less intense than in DMDS, which may be expected because one less C–S orbital is available upon formation of the CH_3S_2 radical. The small peak A_13 in the measured product spectrum is ascribed to these radicals, suggesting minor contributions from asymmetric dissociation.

The spectral changes at the sulfur L_1-edge corroborate a predominant production of methyl-thiyl radicals (Figure 2c,f). The ground-state A1 peak, associated with excitation into the σ^*_{SS} orbital, is absent in the product spectrum and a new peak D1 appears at an energy of ~223 eV. Both effects are very well reproduced by the calculated CH_3S spectrum (red). The observed D1 feature is almost perfectly described by theory and corresponds to an S(2s) → S(3p,SOMO) transition that is absent in the DMDS ground-state spectrum and dipole-forbidden at the sulfur $L_{2,3}$-edge. In contrast, the calculated CH_3S_2 spectrum (dashed green) does not reproduce the observed trends. In particular, it contains a strong A_11 peak, very similar in energy and intensity to the DMDS ground-state A1 peak, which is incompatible with the complete depletion of this peak in the experiment. Moreover, the $S_{1,2}$(3p,SOMO)-associated peaks $D_{1,2}1$ of the CH_3S_2 fragment are much weaker and significantly blue-shifted compared to the measurement. The high-energy shoulder of feature D1 in the measured product spectrum may be associated with D_11 in the calculated CH_3S_2 spectrum, but it is not reproducible among the recorded scans; thus, the assignment is not conclusive.

Photoinduced changes at the carbon K-edge (Figure 2d,g), though more subtle compared to the sulfur L-edges, also support S–S bond cleavage as the dominant initial process. Peaks B and C (corresponding to transitions to σ^*_{CS} and σ^*_{CS}/ryd. orbitals) are affected very little while feature F, associated with excitation to σ^*_{CH} orbitals, grows more intense and is

DOI: 10.1021/acs.jpclett.9b00159
J. Phys. Chem. Lett. 2019, 10, 1382–1387

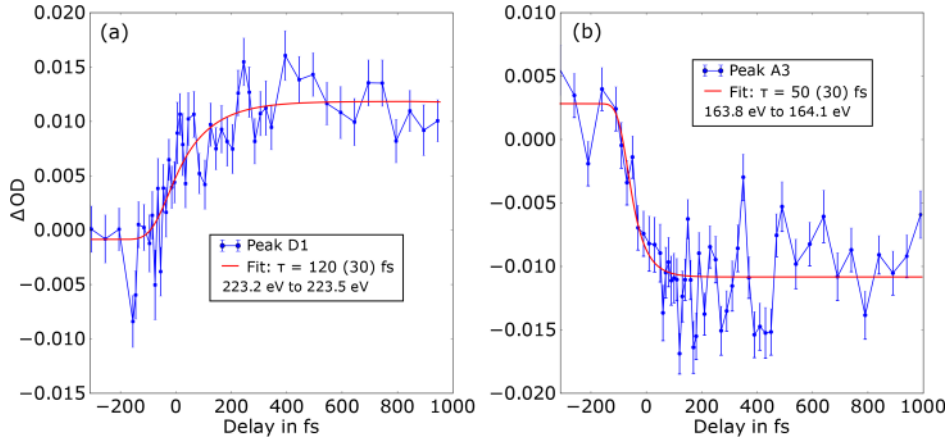

Figure 3. Delay dependence of (a) peak D1 at the sulfur L_1-edge, associated with the formation of CH_3S radicals, recorded with high pump fluence and (b) peak A3 at the sulfur L_3-edge, associated with S−S bond cleavage, recorded with low pump fluence. Each data set is fitted with an exponential rise or decay, convoluted with the instrument response function. Energy integration ranges are noted in the legends.

slightly blue-shifted, which is in line with the calculated CH_3S spectrum. In comparison, the calculated CH_3S_2 + CH_3 spectrum (dashed green) features a weaker peak F with a shoulder at higher energies and peak C is significantly reduced and/or shifted below one of the other features, which is not in agreement with the experiment. The weak feature E originates from the C(1s) → C(2p,SOMO) transitions in CH_3, indicating a minor contribution of asymmetric breakup channels similar to the small $A_1$3 feature at the sulfur $L_{2,3}$-edge. CH_3 carbon K-edge absorption spectra, measured at a synchrotron[21] and in complementary HHG-based experiments on photodissociated CH_3I (Figure S5), yield peak positions of 281.4 and 281.3 eV, respectively, in good agreement with peak E of the measured product spectrum in Figure 3d. The calculated peak E is approximately 2 eV red-shifted compared to the measurement. The relative contribution of CH_3 radicals to the DMDS product spectrum based on this assignment is estimated to be 30 ± 10% by comparing the intensities of peaks B and E in the measured and calculated spectra (Figure S7); however, a significant portion of it is due to multiphoton processes (see below).

The time scale for the CH_3S radical formation can be derived from the integrated intensity of feature D1 (Figure 2c) as a function of the pump−probe delay as shown in Figure 3a. A fit of the measured intensities (blue) with a single exponential rise (red) reveals a radical appearance time of τ = 120 ± 30 fs. Complementary to following the emergence of dissociation products, depletion of the parent ground-state molecule population and cleavage of the S−S bond are also monitored through the decay of the integrated intensity of peak A3 at the sulfur L_3-edge (Figure 3b). A fit of the data with a single exponential decay (red) indicates an overall decay time scale of τ = 50 ± 30 fs. Note that this time scale is shorter than the product appearance time because the parent signal depletion is affected by both electronic structure changes upon photoexcitation and the subsequent coupled electronic−nuclear motion on excited-state potential energy surfaces. A dominant contribution from purely electronic dynamics upon UV excitation, which are instantaneous within the temporal resolution of the experiment, may lead to a change in the signal that is fast compared to the product emergence, which requires notable nuclear motion. Generally, dynamics are probed with the lowest pump intensity possible to suppress potential contributions from multiphoton processes. The emergence of feature D1, however, is derived from higher pump fluence data to achieve a reasonable signal-to-noise ratio. While a high-energy shoulder of D1 is observed at high pump fluences (Figure S8b), it is ensured that this signal does not affect the analysis by selecting only a narrow spectral range around the maximum of feature D1, for which contributions from the shoulder are expected to be negligible. All reported lifetimes take the instrument response into account (eq S5). Peak A2/B3 exhibits the same trend within the experimental uncertainty (Figure S11), strongly indicating that DMDS undergoes direct dissociation into two CH_3S radicals within ∼120 fs.

Comparison of the measured and calculated radical spectra at the sulfur $L_{1,2,3}$- and carbon K-edges strongly suggests that 267 nm photoinduced decomposition of DMDS proceeds predominantly via fragmentation into two CH_3S radicals. However, weak signatures of C−S bond breaking, such as peak $A_1$3 at the sulfur L_3-edge (Figure 2b) and peak E at the carbon K-edge (Figure 2d), indicate that a fraction of parent molecules dissociate asymmetrically into CH_3S_2 and CH_3 fragments. Other possible origins of the small $A_1$3 peak, such as resonances in S_2 products, are ruled out: The lowest-energy transition in S_2 lies ∼1 eV higher than peak $A_1$3, and no further S_2 resonances are observed (Figure S8). Possible production mechanisms of CH_3S_2 and CH_3 radicals are manifold. Using resonance Raman spectroscopy on DMDS with 266 nm excitation, Rinker et al.[10] observed a long progression of C−S stretching modes and, supported by semiempirical calculations, interpreted it as an indicator for molecular breakup at one of the C−S bonds. They furthermore concluded that the lowest electronically excited state is of σ^*_{CS} character, resulting in C−S bond cleavage after 266 nm excitation. In contrast, our CASPT2 calculations find the LUMO to be a σ^*_{SS} orbital, resonantly accessible with 267 nm, and the higher-energetic σ^*_{CS} orbital inaccessible at that wavelength. Other calculations agree that the σ^*_{SS} orbital is the LUMO; however, they find it inaccessible with wavelengths longer than ∼250 nm.[22,23] Therefore, it has been suggested that dissociation at 266 nm into CH_3S_2 and CH_3 must proceed on the electronic ground state.[23] This mechanism, however, typically occurs on pico- to nanosecond time scales and, therefore, can be ruled out by our time-resolved spectra, which find feature E, associated with the

DOI: 10.1021/acs.jpclett.9b00159
J. Phys. Chem. Lett. 2019, 10, 1382−1387

formation of CH_3, to rise within the duration of the <100 fs pump pulse (Figure S13).

While the origin of the asymmetric dissociation cannot be conclusively determined, there are several indications that it may, at least partly, be the result of multiphoton induced processes. Fragmentation into CH_3S_2 + CH_3 radicals has previously been observed in measurements with 133 nm[24,25] and 193 nm[7] excitation. Thus, absorption of two 267 nm photons may access similar dissociation pathways. Fluence-dependent TRXAS measurements and additional calculations (Figure S8) indicate that features X, Y, and Z in the carbon K-edge product spectrum (Figure 2d) are most likely due to multiphoton ionization of DMDS (I_p = 8.2 eV).[25] The same measurements also suggest a multiphoton contribution to peak E, therefore leading to the asymmetric dissociation yield. We note that in a recent picosecond TRXAS study on DMDS in solution at the sulfur K-edge, the authors concluded that C−S bond cleavage is the dominating pathway.[11] However, the experiment employed a pump fluence between the intermediate and highest one used here. Even if there were no secondary reaction processes occurring on picosecond time scales, the results are thus consistent with our findings at higher pump fluences, where multiphoton excitation processes become more prominent.

The results presented here indicate that 267 nm photons excite a nonbonding sulfur electron in DMDS to the antibonding σ^*_{SS} orbital, which leads predominantly to ultrafast dissociation into two methyl-thiyl radicals within ∼120 fs. Asymmetric breakup into CH_3S_2 + CH_3 is also observed with ∼30% relative yield that is at least partly ascribed to multiphoton processes, which are also responsible for the production of $DMDS^+$. The results demonstrate the power of fs-TRXAS to provide real-time insight into the fundamental mechanisms of UV-induced photodamage in molecules containing disulfide bonds, which are key to regulating the structure, function, and stability of biologically relevant molecules such as proteins and enzymes. The atomic-scale perspective provided by deep inner-shell transitions involving sulfur and carbon atoms is well suited for extending the methodologies demonstrated here on a model gas-phase system to larger building blocks of life in both isolation and solution.

■ ASSOCIATED CONTENT

Supporting Information

The Supporting Information is available free of charge on the ACS Publications website at DOI: 10.1021/acs.jpclett.9b00159.

UV absorption spectra, experimental setup, experimental procedures, ground-state absorption spectrum, pump−probe spectra for long delays, complementary CH_3I experiment, product absorption spectra, determination of the content of CH_3 radicals in the DMDS product spectrum, fluence-dependent measurements, absorption spectra of $DMDS^+$ in cis- and trans-configuration, delay-dependent analysis, and computations (PDF)

■ AUTHOR INFORMATION

Corresponding Authors

*E-mail: kirsten.schnorr@psi.ch.
*E-mail: ogessner@lbl.gov.

ORCID

Kirsten Schnorr: 0000-0002-5519-440X
Katherine J. Oosterbaan: 0000-0001-6630-2296
Zheyue Yang: 0000-0002-3446-0860
Adam S. Chatterley: 0000-0003-3847-5936
Martin Head-Gordon: 0000-0002-4309-6669
Stephen R. Leone: 0000-0003-1819-1338

Notes

The authors declare no competing financial interest.

■ ACKNOWLEDGMENTS

K.S. gratefully acknowledges financial support by the Volkswagen foundation. A.B., K.J.O., M.G.D., Z.Y., T.X., A.R.A., M.H.-G., and S.R.L., as well as a portion of the materials and equipment, were supported by the U.S. Department of Energy, Office of Science, Office of Basic Energy Sciences, Chemical Sciences, Geosciences and Biosciences Division under Contract Number DE-AC02-05CH11231, the gas phase chemical physics program through the Chemical Sciences Division of Lawrence Berkeley National Laboratory. O.G. and A.S.C. were funded by the Atomic, Molecular, and Optical Sciences Program, which operates under the same DOE-OS-BES contract number. The apparatus was partially funded by a NSF ERC, EUV Science and Technology, under a previously completed grant (No. EEC-0310717).

■ REFERENCES

(1) Bechtel, T. J.; Weerapana, E. From Structure to Redox: The Diverse Functional Roles of Disulfides and Implications in Disease. *Proteomics* **2017**, *17*, 1600391.

(2) Neves-Petersen, M. T.; Gryczynski, Z.; Lakowicz, J.; Fojan, P.; Pedersen, S.; Petersen, E.; Bjørn Petersen, S. High Probability of Disrupting a Disulphide Bridge Mediated by an Endogenous Excited Tryptophan Residue. *Protein Sci.* **2002**, *11*, 588−600.

(3) Wongkongkathep, P.; Li, H.; Zhang, X.; Loo, R. R. O.; Julian, R. R.; Loo, J. A. Enhancing Protein Disulfide Bond Cleavage by UV Excitation and Electron Capture Dissociation for Top-down Mass Spectrometry. *Int. J. Mass Spectrom.* **2015**, *390*, 137−145.

(4) Martin-Diaconescu, V.; Kennepohl, P. Sulfur K-Edge XAS as a Probe of Sulfur-Centered Radical Intermediates. *J. Am. Chem. Soc.* **2007**, *129*, 3034−3035.

(5) van Gastel, M.; Lubitz, W.; Lassmann, G.; Neese, F. Electronic Structure of the Cysteine Thiyl Radical: A DFT and Correlated ab Initio Study. *J. Am. Chem. Soc.* **2004**, *126*, 2237−2246.

(6) Rao, P. M.; Copeck, J. A.; Knight, A. R. Reactions of Thiyl Radicals. II. The Photolysis of Methyl Disulfide Vapor. *Can. J. Chem.* **1967**, *45*, 1369−1374.

(7) Lee, Y. R.; Chiu, C. L.; Lin, S. M. Ultraviolet Photodissociation Study of CH_3SCH_3 and CH_3SSCH_3. *J. Chem. Phys.* **1994**, *100*, 7376−7384.

(8) Kumar, A.; Chowdhury, P.; Rao, K. R.; Mittal, J. Four-Centered Concerted Ethane Elimination in the IR and UV Laser Photolysis of Dimethyldisulfide. Real-time Observation of S_2 and CH_3S Radicals. *Chem. Phys. Lett.* **1992**, *198*, 406−412.

(9) Hsu, C.; Ng, C. Y. Nonresonant Two-Photon Pulsed Field Ionization of CH_3S Formed in Photodissociation of CH_3SH and CH_3SSCH_3. *J. Chem. Phys.* **1994**, *101*, 5596−5603.

(10) Rinker, A.; Halleman, C. D.; Wedlock, M. R. Photodissociation Dynamics of Dimethyl Disulfide. *Chem. Phys. Lett.* **2005**, *414*, 505−508.

(11) Ochmann, M.; Hussain, A.; von Ahnen, I.; Cordones, A. A.; Hong, K.; Lee, J. H.; Ma, R.; Adamczyk, K.; Kim, T. K.; Schoenlein, R. W.; Vendrell, O.; Huse, N. UV-Photochemistry of the Disulfide Bond: Evolution of Early Photoproducts from Picosecond X-ray

DOI: 10.1021/acs.jpclett.9b00159
J. Phys. Chem. Lett. 2019, 10, 1382−1387

Absorption Spectroscopy at the Sulfur K-Edge. *J. Am. Chem. Soc.* **2018**, *140*, 6554−6561.
(12) Wenzel, J.; Wormit, M.; Dreuw, A. Calculating Core-Level Excitations and X-ray Absorption Spectra of Medium-Sized Closed-Shell Molecules with the Algebraic-Diagrammatic Construction Scheme for the Polarization Propagator. *J. Comput. Chem.* **2014**, *35*, 1900−1915.
(13) Dunning, T. H., Jr. Gaussian Basis Sets for Use in Correlated Molecular Calculations. I. The Atoms Boron through Neon and Hydrogen. *J. Chem. Phys.* **1989**, *90*, 1007−1023.
(14) Woon, D. E.; Dunning, T. H., Jr. Gaussian Basis Sets for Use in Correlated Molecular Calculations. III. The Atoms Aluminum through Argon. *J. Chem. Phys.* **1993**, *98*, 1358−1371.
(15) Andersson, K.; Malmqvist, P.; Roos, B. O. Second-Order Perturbation Theory with a Complete Active Space Self-Consistent Field Reference Function. *J. Chem. Phys.* **1992**, *96*, 1218−1226.
(16) Malmqvist, P.; Pierloot, K.; Shahi, A. R. M.; Cramer, C. J.; Gagliardi, L. The Restricted Active Space Followed by Second-Order Perturbation Theory Method: Theory and Application to the Study of CuO_2 and Cu_2O_2 Systems. *J. Chem. Phys.* **2008**, *128*, 204109.
(17) Roos, B. O.; Lindh, R.; Malmqvist, P.; Veryazov, V.; Widmark, P.-O. Main Group Atoms and Dimers Studied with a New Relativistic ANO Basis Set. *J. Phys. Chem. A* **2004**, *108*, 2851−2858.
(18) Malmqvist, P.; Roos, B. O.; Schimmelpfennig, B. The Restricted Active Space (RAS) State Interaction Approach with Spin-Orbit Coupling. *Chem. Phys. Lett.* **2002**, *357*, 230−240.
(19) Bernini, R. B.; da Silva, L. B. G.; Rodrigues, F. N.; Coutinho, L. H.; Rocha, A. B.; de Souza, G. G. B. Core Level (S *2p*) Excitation and Fragmentation of the Dimethyl Sulfide and Dimethyldisulfide Molecules. *J. Chem. Phys.* **2012**, *136*, 144307.
(20) Baba, Y.; Yoshii, K.; Sasaki, T. A. Site-Specific Fragmentation in Condensed $(CH_3S_2)_2$ by Sulfur K-Edge Photoexcitation. *J. Chem. Phys.* **1996**, *105*, 8858−8864.
(21) Alagia, M.; Lavollée, M.; Richter, R.; Ekström, U.; Carravetta, V.; Stranges, D.; Brunetti, B.; Stranges, S. Probing the Potential Energy Surface by High-Resolution X-ray Absorption Spectroscopy: The Umbrella Motion of the Core-Excited CH_3 Free Radical. *Phys. Rev. A: At., Mol., Opt. Phys.* **2007**, *76*, 022509.
(22) Rauk, A. Chiroptical Properties of Disulfides. Ab Initio Studies of Dihydrogen Disulfide and Dimethyl Disulfide. *J. Am. Chem. Soc.* **1984**, *106*, 6517−6524.
(23) Luo, C.; Du, W.-N.; Duan, X.-M.; Liu, J.-Y.; Li, Z.-S. Theoretical Study on the Excited States and Photodissociation Mechanism of Dimethyldisulfide. *Chem. Phys. Lett.* **2009**, *469*, 242−246.
(24) Butler, J. J.; Baer, T.; Evans, S. A. Energetics and Structures of Organosulfur Ions: $CH_3SSCH_3^+$, CH_3SS^+, $C_2H_5S^+$, and CH_2SH^+. *J. Am. Chem. Soc.* **1983**, *105*, 3451−3455.
(25) Chiang, S.-Y.; Ma, C.-I.; Shr, D.-J. Dissociative Photoionization of CH_3SSCH_3 in the Region of ∼ 8−25 eV. *J. Chem. Phys.* **1999**, *110*, 9056−9063.

DOI: 10.1021/acs.jpclett.9b00159
J. Phys. Chem. Lett. 2019, 10, 1382−1387